

Consistent mean-field description of the $^{12}\text{C}+^{12}\text{C}$ optical potential at low energies and the astrophysical S factor

Le Hoang Chien^{1,2}, Dao T. Khoa^{1,*}, Do Cong Cuong¹, and Nguyen Hoang Phuc¹

¹ *Institute for Nuclear Science and Technology, VINATOM
179 Hoang Quoc Viet, Cau Giay, Hanoi, Vietnam.*

² *Department of Nuclear Physics and Nuclear Engineering,
Faculty of Physics and Engineering Physics, University of Science, VNU-HCM,
227 Nguyen Van Cu, District 5, Ho Chi Minh City, Vietnam.*

(Dated: December 14, 2018)

Abstract

The nuclear mean-field potential built up by the $^{12}\text{C}+^{12}\text{C}$ interaction at energies relevant for the carbon burning process is calculated in the double-folding model (DFM) using the realistic ground-state density of ^{12}C and the CDM3Y3 density dependent nucleon-nucleon (NN) interaction, with the rearrangement term properly included. To validate the use of a density dependent NN interaction in the DFM calculation in the low-energy regime, an adiabatic approximation is suggested for the nucleus-nucleus overlap density. The reliability of the nuclear mean-field potential predicted by this low-energy version of the DFM is tested in a detailed optical model analysis of the elastic $^{12}\text{C}+^{12}\text{C}$ scattering data at energies below 10 MeV/nucleon. The folded mean-field potential is then used to study the astrophysical S factor of $^{12}\text{C}+^{12}\text{C}$ fusion in the barrier penetration model. Without any adjustment of the potential strength, our results reproduce very well the non-resonant behavior of the S factor of $^{12}\text{C}+^{12}\text{C}$ fusion over a wide range of energies.

PACS numbers:

*Electronic address: khoa@vinatom.gov.vn

I. INTRODUCTION

The $^{12}\text{C}+^{12}\text{C}$ reaction plays an important role in the chain of the nucleosynthesis processes during stellar evolution, as the main nuclear reaction governing the carbon burning process in massive stars [1, 2]. For example, the $^{12}\text{C}+^{12}\text{C}$ reaction has a significant impact on the evolution and structure of massive stars with $M \gtrsim 8M_{\odot}$ [2–4], where a large concentration of the ^{12}C ashes built up after the helium burning stage leads directly to the $^{12}\text{C}+^{12}\text{C}$ fusion that yields heavier nuclei such as ^{23}Na , ^{20}Ne , and ^{23}Mg for the next burning stage of the stellar evolution. In a young massive star with $M \lesssim 8M_{\odot}$, $^{12}\text{C}+^{12}\text{C}$ fusion is also known as the pycnonuclear reaction that reignites a carbon-oxygen white dwarf into a type Ia supernova explosion. Because of the astrophysical importance of $^{12}\text{C}+^{12}\text{C}$ fusion at low energies, many experimental and theoretical efforts have been made in the last forty years to understand the reaction mechanism and to obtain as accurately as possible the $^{12}\text{C}+^{12}\text{C}$ reaction cross section down to the Gamow energy of about 1.5 MeV [5–25].

The tremendous challenge for the experimental study of $^{12}\text{C}+^{12}\text{C}$ fusion at energies relevant for stellar conditions is that this reaction occurs at very low energies of about 1 to 3 MeV, determined by the stellar thermal energy, while the Coulomb barrier for this system is around 7 MeV. This makes the direct measurement in the laboratory extremely difficult when trying to obtain accurate data of the $^{12}\text{C}+^{12}\text{C}$ fusion cross section in the Gamow energy region (on the order of a nanobarn or lower) [23, 24], which is the important input for nuclear astrophysics studies. In these studies, one usually needs to extrapolate the $^{12}\text{C}+^{12}\text{C}$ fusion cross section to the low-energy regime based on the experimental data available at higher energies. However, uncertainties in such a procedure remain very significant [3] due to the resonant structure of the $^{12}\text{C}+^{12}\text{C}$ reaction cross section as well as the considerable discrepancy between the data sets obtained from different measurements in the same energy range, and the uncertainties of these measurements which are very large at the lowest energies (see, e.g., Fig. 1 of Ref. [24]). Therefore, a reliable theoretical prediction of the $^{12}\text{C}+^{12}\text{C}$ fusion cross section down to the Gamow energy should be of high astrophysical interest. For this purpose, several theoretical studies have been performed to describe $^{12}\text{C}+^{12}\text{C}$ fusion; which such studies were based mainly on the semiclassical barrier penetration model (BPM). The description of the $^{12}\text{C}+^{12}\text{C}$ fusion cross section in the BPM depends strongly on the choice of the $^{12}\text{C}+^{12}\text{C}$ interaction potential [14, 18, 21, 22, 26–28].

In general, the validity of a potential model for the description of the $^{12}\text{C}+^{12}\text{C}$ interaction at sub-Coulomb energies should first be tested in a consistent optical model (OM) analysis of the elastic $^{12}\text{C}+^{12}\text{C}$ scattering at low energies. In fact, the measurements of the $^{12}\text{C}+^{12}\text{C}$ scattering and reaction have been performed over a wide range of energies during the last 40 years. In particular, in the energy region below 10 MeV/nucleon there exist several data sets of elastic $^{12}\text{C}+^{12}\text{C}$ scattering [29–34] that can be used in the OM analysis to probe different potential models. We must note that this is not a simple task because of the ambiguity of the optical potential (OP) often found in the OM studies of the elastic light heavy-ion (HI) scattering at low energies. For example, a very shallow real OP was frequently deduced from the OM analyses of the elastic $^{16}\text{O}+^{16}\text{O}$, $^{14}\text{N}+^{14}\text{N}$, and $^{12}\text{C}+^{12}\text{C}$ scattering in the energy region below 6 MeV/nucleon [35–37]. For the $^{12}\text{C}+^{12}\text{C}$ system, the OM analyses of the elastic scattering at bombarding energies of 35 to 75 MeV seem to prefer a shallow Woods-Saxon (WS) real OP with a depth of around 14 MeV [29, 37]. In contrast, the OM studies of the elastic $^{12}\text{C}+^{12}\text{C}$ scattering at higher energies have shown unambiguously that the measured elastic $^{12}\text{C}+^{12}\text{C}$ scattering cross sections imply the use of a deep real OP that can be obtained from the double-folding model (DFM) or parametrized in the WS or WS-squared forms [38–40]. In some particular cases, both the shallow and deep WS potentials were found to give about the same OM description of the elastic $^{12}\text{C}+^{12}\text{C}$ data at forward angles $\theta_{\text{c.m.}} \lesssim 50^\circ$ in the center-of-mass (c.m.) frame. However, the shallow real OP usually failed to account for the data points measured at larger angles, $50^\circ \lesssim \theta_{\text{c.m.}} \lesssim 100^\circ$ [31].

In this connection, it is necessary to draw the reader’s attention to the mean-field nature of the light HI interaction [40, 41]. Namely, it has been shown [41] that the mean-field potential built up from the $^{12}\text{C}+^{12}\text{C}$ interaction smoothly matches the deep family of the real OP that gives consistently a good OM description of the elastic $^{12}\text{C}+^{12}\text{C}$ scattering from medium energies down to those near the Coulomb barrier. On the Hartree-Fock (HF) level, such a mean-field potential is readily obtained in the double-folding model [40, 42–48] using the ground-state (g.s.) densities of the two colliding nuclei and a realistic *density dependent* nucleon-nucleon (NN) interaction. At medium energies, the real OP given by the DFM was proved to account properly for the nuclear rainbow pattern observed in elastic light HI scattering [40, 47, 48]. Not only an interesting (analogous to an atmospheric rainbow) phenomenon, the observation of the nuclear rainbow also allows one to determine the strength and shape of the real OP down to small internuclear distances [47]. In a smooth extrapola-

tion of the mean-field potential to the low-energy region, the deep folded potential was shown [41] to give sufficient numbers of nodes in the relative-motion wave function as implied by the Pauli principle and to provide a natural explanation of the low-energy resonances in the $^{12}\text{C}+^{12}\text{C}$ system and their relation to the cluster model of ^{24}Mg . This is a strong indication that the DFM can be used as a good potential model for the description of $^{12}\text{C}+^{12}\text{C}$ fusion at astrophysical energies. However, in a nucleus-nucleus collision at very low energies the dinuclear medium is formed more or less adiabatically with much less compression, and the dinuclear overlap density needs to be treated properly before the DFM can be used with a realistic density dependent NN interaction. This issue has not been investigated so far, and a simple version of the DFM using some *density independent* NN interaction is usually used to calculate the nucleus-nucleus potential for the description of the $^{12}\text{C}+^{12}\text{C}$ fusion at low energies (see, e.g., Refs. [14, 22]).

Instead of the frozen density approximation widely used in the DFM calculation of the nucleus-nucleus potential at energies above 10 MeV/nucleon [45, 47, 48], we propose in the present work an adiabatic approximation for the dinuclear overlap density, similar to that suggested years ago by Reichstein and Malik [49, 50] in their study of nuclear fission. This adiabatic density approximation (ADA) is then used in the new version of the DFM [48] that properly includes also the nucleon rearrangement term, to predict the nuclear mean-field potential built up in the $^{12}\text{C}+^{12}\text{C}$ collision at low energies. The reliability of the folded $^{12}\text{C}+^{12}\text{C}$ potential predicted by the present DFM calculation is carefully tested in the OM analysis of the elastic $^{12}\text{C}+^{12}\text{C}$ scattering over a wide range of energies below 10 MeV/nucleon. Given the nuclear astrophysical importance of $^{12}\text{C}+^{12}\text{C}$ fusion, the mean-field folded potential obtained for the $^{12}\text{C}+^{12}\text{C}$ system is further used in the BPM to study the (non-resonant) energy dependent behavior of the astrophysical S factor and reaction rate of the $^{12}\text{C}+^{12}\text{C}$ fusion down to the Gamow energy. The CDM3Y3 density dependent NN interaction has been used to obtain a realistic HF description of nuclear matter as well as the nucleon mean-field potential at different densities of the nuclear medium [51], and the consistent DFM determination of the $^{12}\text{C}+^{12}\text{C}$ interaction potential at low energies using this same interaction is, therefore, well founded. Thus, it is natural to expect that the mean-field $^{12}\text{C}+^{12}\text{C}$ potential predicted by this low-energy version of the DFM can be used as a reliable input for the BPM study of stellar carbon burning.

II. DFM AND ELASTIC $^{12}\text{C}+^{12}\text{C}$ SCATTERING AT LOW ENERGIES

As mentioned above, the earlier OM analyses of the elastic $^{12}\text{C}+^{12}\text{C}$ scattering at low energies often show an ambiguity of the OP, when both the shallow and deep real optical potentials give nearly the same satisfactory description of the elastic scattering data, especially, for the data points taken at forward angles ($\theta_{c.m.} \lesssim 50^\circ$). Only with the high-precision data measured at larger angles, does the choice of a deep real OP seem to be more appropriate for a good OM description of the elastic $^{12}\text{C}+^{12}\text{C}$ scattering data over the whole angular range. The deep family of the real OP for the $^{12}\text{C}+^{12}\text{C}$ system was shown to be close, in strength and shape, to the mean-field potential predicted by the DFM [43–48]. Given the improved version of the DFM with a proper treatment of the rearrangement term [48], it is of interest to probe the reliability of the DFM in the OM study of elastic $^{12}\text{C}+^{12}\text{C}$ scattering at low energies, and the further use of the folded potential to estimate the astrophysical S factor of the $^{12}\text{C}+^{12}\text{C}$ fusion in the BPM calculation. For this purpose, we have chosen several data sets [9, 29, 31, 37] of the elastic $^{12}\text{C}+^{12}\text{C}$ angular distributions and excitation functions measured at energies ranging from the Coulomb barrier up to around 10 MeV/nucleon.

We recall that in the DFM the nucleus-nucleus OP at the given internuclear distance R is evaluated as a HF-type potential [44, 45, 47] using an effective (energy- and density dependent) NN interaction $v(\rho, E)$:

$$V(E, R) = \sum_{i \in a, j \in A} [\langle ij | v_D(\rho, E) | ij \rangle + \langle ij | v_{EX}(\rho, E) | ji \rangle], \quad (1)$$

where $|i\rangle$ and $|j\rangle$ are the single-nucleon wave functions of the projectile (a) and target (A) nucleons, respectively. The direct part of the double-folded potential (1) is local, and can be evaluated using the g.s. densities of the two colliding nuclei as

$$V_D(E, R) = \int \rho_a(\mathbf{r}_a) \rho_A(\mathbf{r}_A) v_D(\rho, E, s) d^3 r_a d^3 r_A, \quad \mathbf{s} = \mathbf{r}_A - \mathbf{r}_a + \mathbf{R}. \quad (2)$$

The antisymmetrization of the $a + A$ system (the knock-on exchange effect) results in the exchange term V_{EX} that is nonlocal in the coordinate space. A local approximation is usually made using the WKB treatment of the relative-motion wave function [47] to obtain the exchange term of the folded potential (1) in the local form

$$V_{EX}(E, R) = \int \rho_a(\mathbf{r}_a, \mathbf{r}_a + \mathbf{s}) \rho_A(\mathbf{r}_A, \mathbf{r}_A - \mathbf{s}) \times v_{EX}(\rho, E, s) \exp\left(\frac{i\mathbf{K}(E, R) \cdot \mathbf{s}}{M}\right) d^3 r_a d^3 r_A, \quad (3)$$

where $\rho_{a(A)}(\mathbf{r}, \mathbf{r}')$ are the nonlocal g.s. density matrices, $M = aA/(a + A)$ is the recoil factor (or reduced mass number); a and A are the mass numbers of the projectile and target, respectively. The local (energy dependent) relative momentum $K(E, R)$ is determined self-consistently from the real OP as

$$K^2(E, R) = \frac{2\mu}{\hbar^2}[E - V(E, R) - V_C(R)], \quad (4)$$

where μ is the reduced mass of the two nuclei. The Coulomb potential $V_C(R)$ is obtained by directly folding two uniform charge distributions [52], chosen to have a RMS charge radius $R_C = 3.17$ fm for ^{12}C . Such a choice of the Coulomb potential was shown to be accurate up to small internuclear distances [40].

For the effective NN interaction, we have used in the present work the CDM3Y3 density dependent version [44] of the original M3Y-Paris interaction that is based on the G-matrix elements of Paris potential [53].

$$v_{\text{D(EX)}}(\rho, E, s) = g(E)F(\rho)v_{\text{D(EX)}}(s). \quad (5)$$

The radial parts of the direct and exchange terms $v_{\text{D(EX)}}(s)$ were kept unchanged as given in terms of three Yukawas potentials by the spin- and isospin independent part of the M3Y-Paris interaction [53]. The density dependent functional $F(\rho)$ in Eq. (5) was first suggested in Ref. [44], where its parameters were chosen to correctly reproduce the saturation properties of cold nuclear matter and give a realistic value of the nuclear incompressibility $K \approx 217$ MeV in the HF calculation of nuclear matter (see, e.g., Fig. 1 in Ref. [48]). The $g(E)$ factor accounts for the in-medium energy dependence of the CDM3Y3 interaction (5), and is determined self-consistently [48] using the local relative momentum (4).

In the HF calculation of finite nuclei using a density dependent NN interaction, there appears naturally a rearrangement term (RT) in the HF energy density which corresponds to the rearrangement of the mean field caused by the removal or addition of a single nucleon [54]. The significant impact of the RT was shown experimentally in the direct nucleon transfer reactions at low energies [55]. In the same manner, the RT must appear in the HF-type folding model calculation of the nucleon-nucleus or nucleus-nucleus potential using explicitly a density dependent NN interaction and single-nucleon wave functions of the projectile and target nucleons. This important aspect of the folding model was investigated recently [48, 51], and it was shown that the contribution of the RT to the folded potential (1)-(4)

can be accurately accounted for by adding a density dependent correction term $\Delta F(\rho)$ to the density dependence $F(\rho)$ of the CDM3Y3 interaction, i.e., instead of (5),

$$v_{\text{D(EX)}}(\rho, E, s) = g(E)[F(\rho) + \Delta F(\rho)]v_{\text{D(EX)}}(s) \quad (6)$$

is used in the DFM calculation (2) and (4) of the nucleus-nucleus OP. We obtain then the contribution of the RT to the total folded potential explicitly as

$$V(E, R) = V_{\text{HF}}(E, R) + V_{\text{RT}}(E, R), \quad (7)$$

where V_{HF} and V_{RT} are the HF-type and rearrangement terms of the double-folded potential (1), respectively. In the present work we have used the g.s. density of ^{12}C obtained recently in a microscopic no-core shell model (NCSM) calculation [56] which reproduces nicely the empirical matter radius of ^{12}C . All the OM analyses were made using the code ECIS97 written by Raynal [57]. More details on the new DFM with the inclusion of the RT and explicit parameters (6) of the CDM3Y3 interaction can be found in Ref. [48].

Adiabatic density approximation

Because the strength and shape of the double-folded potential at small radii depends strongly on the dinuclear overlap density at these distances [47], the treatment of the nucleus-nucleus overlap is an important procedure in a DFM calculation using a density dependent NN interaction. The most used approximation so far is the frozen density approximation (FDA), where the sum of two “frozen” g.s. densities is used to determine the overlap density ρ appearing in Eq. (6). The validity of the FDA was discussed repeatedly in the past [42–44, 46, 47], and it has been proven to be a reliable approximation at energies above 10 MeV/nucleon (see, e.g., the results of a quantum molecular dynamics simulation of the $^{16}\text{O}+^{16}\text{O}$ collision at 22 MeV/nucleon [43] where the dinuclear overlap density during the compression is very close to that given by the FDA). At low energies of sub-barrier fusion, the dinuclear system is transformed adiabatically into a compound nucleus [58–61] with decreasing internuclear distance R , and the FDA or sudden approximation for the overlap density is no longer valid. The compression of the overlap region is also much weaker than that established in nucleus-nucleus collisions at medium and high energies. Therefore, the nucleus-nucleus overlap density needs to be treated in a proper adiabatic approximation before the DFM can be used to estimate the nucleus-nucleus OP in this energy regime.

In the present work, we propose a prescription to determine the overlap density similar to the adiabatic density approximation suggested some 40 years ago by Reichstein and Malik [49, 50] for the compound density formed in a HI collision at low energies [49] or that at the onset of nuclear fission [50]. The only attempt to use such an ADA in the microscopic calculation of the $^{12}\text{C}+^{12}\text{C}$ optical potential was done by Ohtsuka *et al.* [62] in the energy density formalism. Based on the recent results of systematic investigations of sub-barrier fusion [59–61], the $^{12}\text{C}+^{12}\text{C}$ overlap density is assumed to change gradually from that given by the FDA to that given by the ADA with decreasing distance R , so that the total overlap density approaches the central density of ^{24}Mg at zero distance. Namely, the $^{12}\text{C}+^{12}\text{C}$ overlap density is given by the sum of the two carbon densities ρ_C determined at the given internuclear separation R as

$$\rho_C(r) = \begin{cases} 0.5 \rho_{\text{Mg}}(r) \exp \left[\ln \left(\frac{\rho_0(r)}{0.5 \rho_{\text{Mg}}(r)} \right) \left(\frac{R}{R_{\text{cut}}} \right) \right] & \text{if } R \leq R_{\text{cut}} \\ \rho_0(r) & \text{if } R > R_{\text{cut}}, \end{cases} \quad (8)$$

where R_{cut} is the grazing distance at which two nuclei begin to overlap. ρ_0 and ρ_{Mg} are the g.s. densities of ^{12}C and ^{24}Mg , respectively. We note that the total nucleon number given by the density distribution (8) at any distance is conserved ($A = 12$). The g.s. density of ^{24}Mg is taken from the results of the Hartree-Fock-Bogoliubov calculation [63]. For the grazing distance, we choose $R_{\text{cut}} \approx 6$ fm for the $^{12}\text{C}+^{12}\text{C}$ system which is very close to the touching distance given by the extended coupled channel analysis of the sub-barrier fusion [59, 61], where the potential energy of the system is determined based on a smooth transition from the sudden- to the adiabatic approximation. The $^{12}\text{C}+^{12}\text{C}$ overlap densities given by the two approximations at different distances R are shown in Fig. 1. While the FDA gives the total overlap density at small separation distances up to twice the central density of ^{12}C , that given by the ADA is much lower and approaches closely the central density of ^{24}Mg . The use of the ADA results naturally in a less repulsion in the nucleus-nucleus interaction at small radii, and the double-folded potential obtained using the ADA approximation becomes more attractive in the center compared to that obtained using the FDA. The difference of the two approximations for the overlap density affects the strength and slope of the double-folded potential significantly at small radii (see three versions of the double-folded $^{12}\text{C}+^{12}\text{C}$ potential shown in Fig. 2). In the discussion hereafter, we denote the HF-type potential V_{HF} obtained using the FDA as DF1, the total double-folded $V_{\text{HF}} + V_{\text{RT}}$ potential obtained

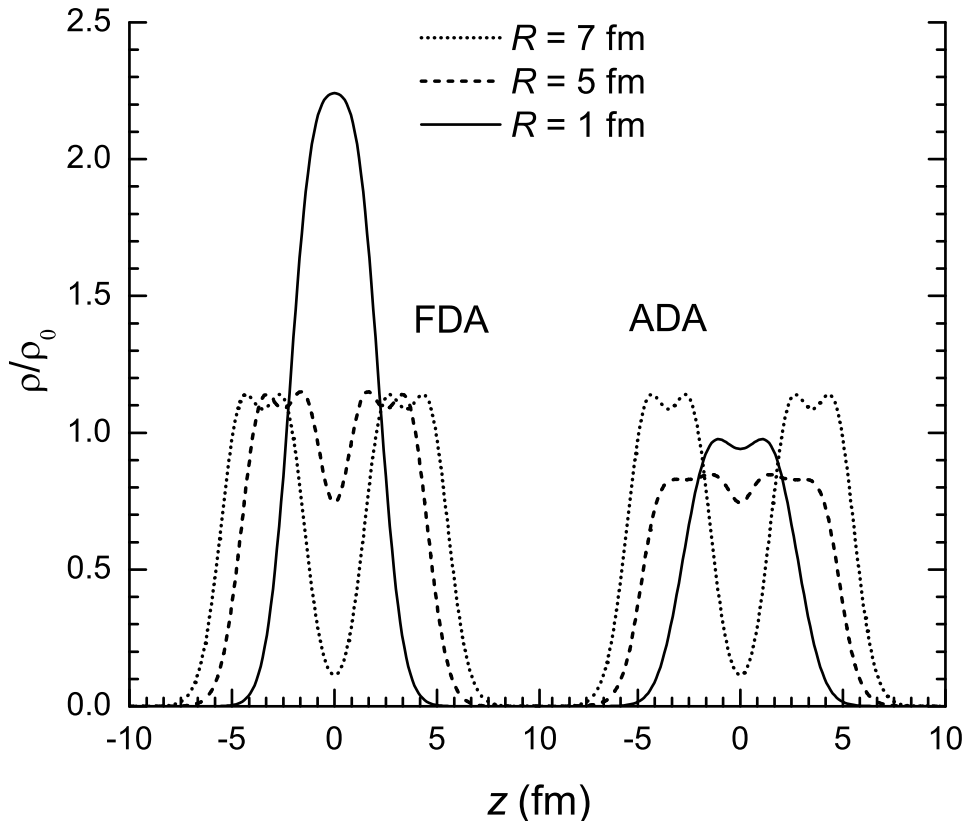


FIG. 1: The $^{12}\text{C}+^{12}\text{C}$ overlap density given by the FDA and ADA (in ratio to the saturation density of nuclear matter $\rho_0 \approx 0.17 \text{ fm}^{-3}$) at different internuclear distances R . The z axis is along the line connecting the centers of the two ^{12}C nuclei.

using the FDA as DF2, and the total potential obtained using the ADA as DF3. One can see that the difference between the DF2 and DF3 potentials at $R < R_{\text{cut}}$ is very significant. The DF3 potential has a larger slope in the interior region and is about 90 MeV deeper than the DF2 potential in the center. Beyond the grazing radius, the two potentials DF2 and DF3 have the same strength at the surface. As shown recently for the nucleon-nucleus and nucleus-nucleus folded potentials [48, 51], the rearrangement term gives rise to a strong repulsive contribution of the RT to the folded potential at small radii, and this leads to the difference between the DF1 and DF2 potentials shown in Fig. 2.

The OM description of the elastic $^{12}\text{C}+^{12}\text{C}$ scattering data at $E_{\text{lab}} = 78.8 \text{ MeV}$ using the three versions of the double-folded potential as the real OP is shown in Fig. 3. The imaginary OP has been assumed to be in the WS form with the parameters adjusted by

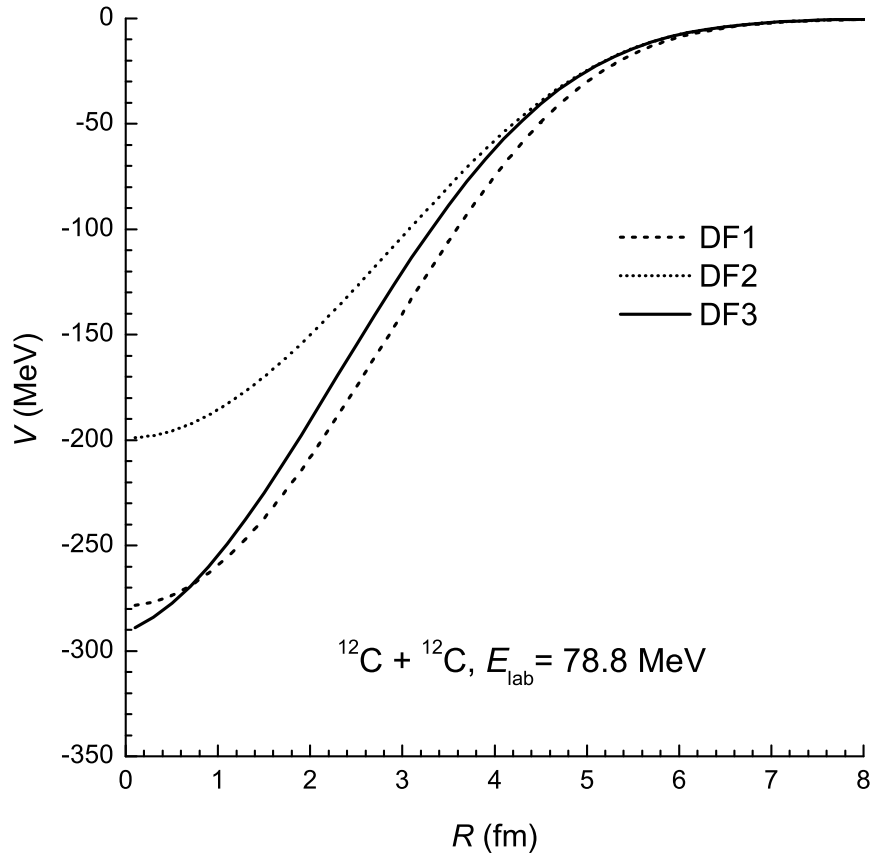


FIG. 2: Three versions of the double-folded $^{12}\text{C}+^{12}\text{C}$ potential (7) obtained at $E_{\text{lab}} = 78.8 \text{ MeV}$ using either the FDA or ADA for the overlap density. DF1 is the V_{HF} potential based on the FDA, DF2 is the $V_{\text{HF}} + V_{\text{RT}}$ potential based on the FDA, and DF3 the is $V_{\text{HF}} + V_{\text{RT}}$ potential based on the ADA.

the best OM description of the elastic data at forward angles, which are sensitive to the strength of the OP at the surface. The starting values for this OM fit were taken from the global OP for elastic $^{12}\text{C}+^{12}\text{C}$ scattering at higher energies [39], and the best-fit WS parameters obtained with the three types of the real double-folded OP are quite close (see, e.g., the WS parameters obtained with the DF3 potential given in Table I). Figure 3 shows that the difference in the real double-folded OPs at small radii can be seen clearly in the calculated elastic cross section at large angles. From the OM results obtained with the DF2 and DF3 real OPs which were given, respectively, by the FDA and ADA treatments of the overlap density, it can be concluded that the ADA is more appropriate for the overlap density used in the DFM calculation at low energies. Without the renormalization of the potential

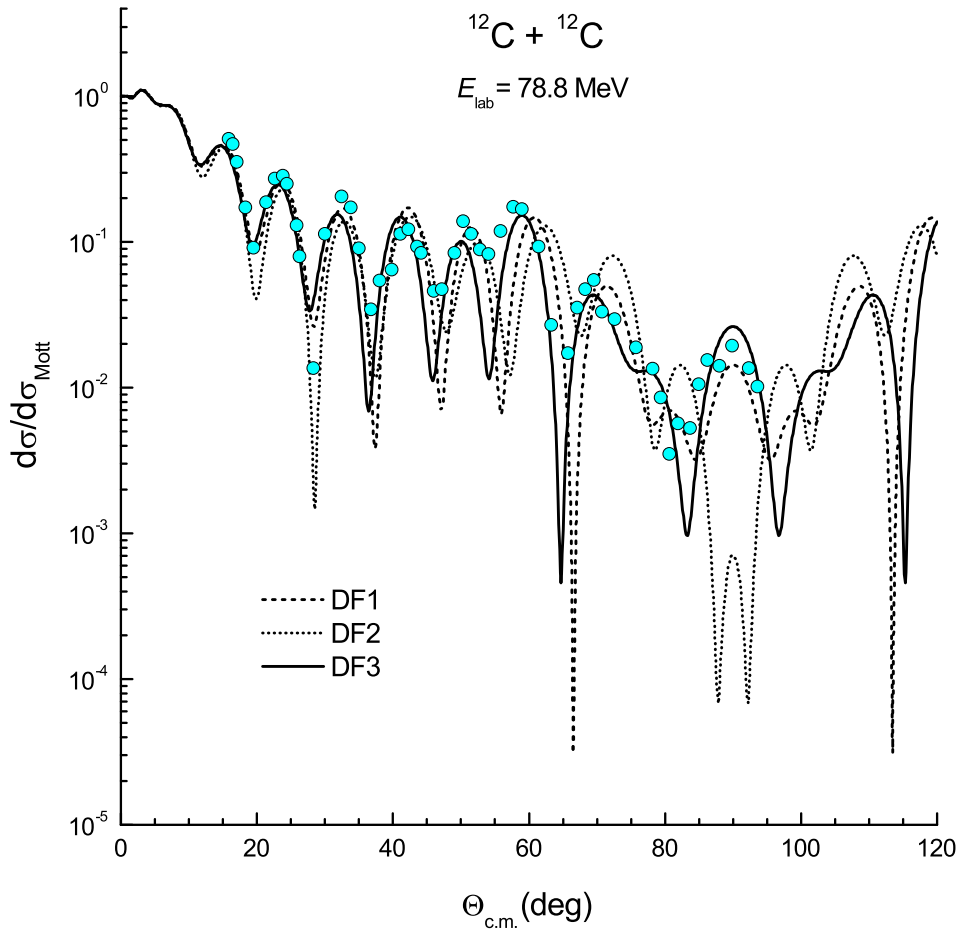


FIG. 3: OM description of the elastic $^{12}\text{C}+^{12}\text{C}$ scattering data at $E_{\text{lab}} = 78.8$ MeV given by three versions of the real double-folded $^{12}\text{C}+^{12}\text{C}$ potential shown in Fig. 2 and the WS imaginary potential with parameters given in Table I. $N_{\text{R}} = 1$ was used with the folded potentials.

strength, from three versions of the double-folded potential only the DF3 potential (given by the ADA) accounts well for the measured elastic data over the whole angular range. At small radii the DF3 potential has a depth very close to the WS depth of 280 MeV fixed by the phenomenological OM and coupled-channel analyses of the low-energy elastic $^{12}\text{C}+^{12}\text{C}$ scattering [64]. The use of the FDA leads to the shallower DF2 potential which is unable to account for the measured elastic data at large angles, even when a renormalization N_{R} of its strength is introduced as a fitting parameter in the OM calculation. When the RT is neglected, the DF1 potential (given by the FDA) has about the same depth as that of the DF3 potential, but is more attractive at the surface as shown in Fig. 2. As a result, the

DF1 potential needs to be renormalized by $N_R \approx 0.8$ for a reasonable OM description of the data over the whole angular range, and this accounts roughly for the missing repulsive contribution of the RT to the folded potential as discussed in Refs. [48] and [51].

Results of the OM analysis and discussion

To probe the validity of the present (low-energy) version of the DFM, we have performed a detailed OM analysis of the elastic $^{12}\text{C}+^{12}\text{C}$ scattering data at energies of 1.3 to 10 MeV/nucleon [9, 29, 31, 37]. The double-folded potential (7) was used as the real OP and the imaginary OP was assumed to be in the standard WS form, so that the total OP at the internuclear distance R is determined as

$$U(R) = N_R V(E, R) - \frac{iW_V}{1 + \exp[(R - R_V)/a_V]} + V_C(R). \quad (9)$$

Usually the renormalization factor N_R of the real double-folded potential (7) is used to effectively account for the higher-order (beyond mean-field) contribution of the dynamic polarization potential (DPP) to the microscopic nucleus-nucleus OP [40, 47]. At energies of astrophysical interest, most of the nonelastic channels are closed and the DPP contribution should be weak enough for N_R to be kept at unity. When the ingredients of the DFM are appropriately chosen, the OM calculation with $N_R \approx 1$ should give a good description of the considered elastic scattering data. Therefore, we have kept $N_R = 1$ throughout the present work to test the reliability of the double-folded potential in the OM analysis of the elastic $^{12}\text{C}+^{12}\text{C}$ scattering at low energies. The WS parameters of the imaginary OP were adjusted by the best OM fit to the elastic data at forward angles as discussed above for the data at 78.8 MeV, starting from parameters of the global OP for elastic $^{12}\text{C}+^{12}\text{C}$ scattering at higher energies [39, 40]. For the considered elastic data, the best-fit WS parameters obtained with the three double-folded potentials are quite close, giving about the same volume integral J_W and total reaction cross section σ_R as those given in Table I.

The results of our folding model analysis of the elastic $^{12}\text{C}+^{12}\text{C}$ scattering at $E_{\text{lab}} = 16 - 117$ MeV are shown in Figs. 4, 5, and 6. At the low energy $E_{\text{lab}} = 16$ MeV, the elastic scattering occurs mainly at the surface and deviates from the Coulomb scattering only at large angles around $80 - 90^\circ$, and the three versions of the double-folded potential give more or less the same OM description of the data. With increasing energies, the DF1

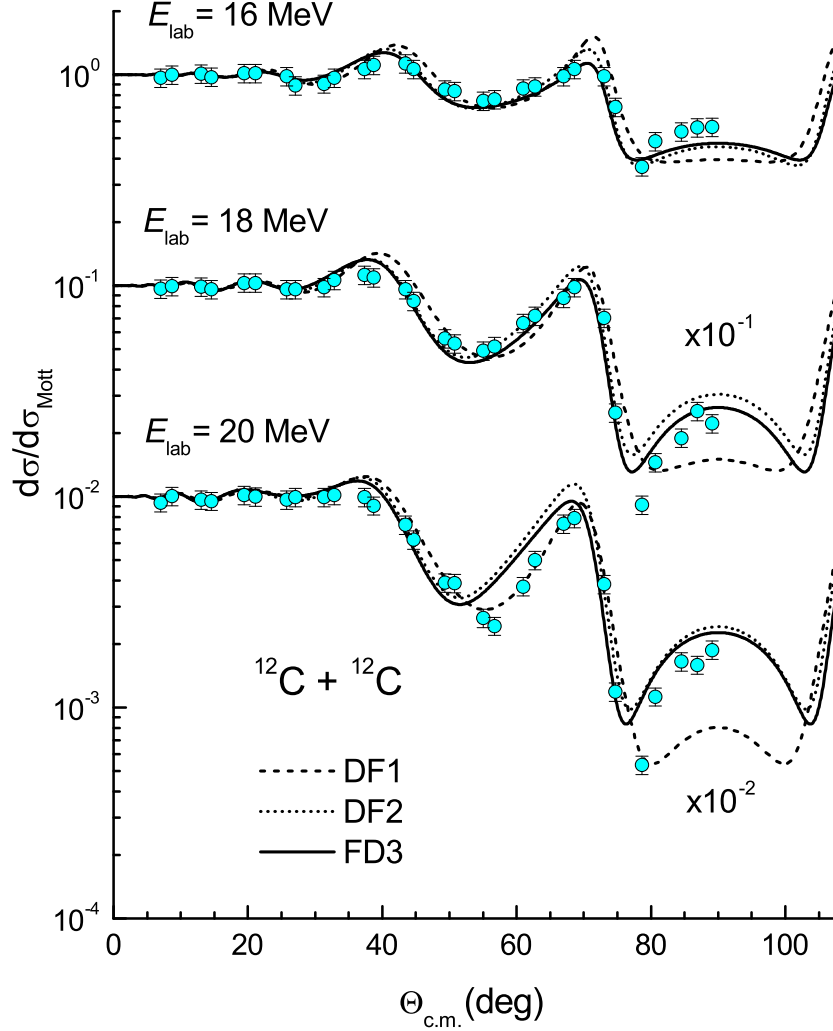


FIG. 4: OM descriptions of the elastic $^{12}\text{C}+^{12}\text{C}$ scattering data at $E_{\text{lab}} = 16, 18,$ and 20 MeV [9] given by three versions of the real OP considered in the present work. The same notation as that in Fig. 2 is used for the double-folded potential

potential (with a too attractive strength at the surface) fails to account for the large-angle data (see Fig. 4). The DF2 and DF3 potentials are the same up to the grazing distance of $R = 6$ fm, and they give equally good OM descriptions of the elastic data at energies up to $E_{\text{lab}} = 20$ MeV. At higher energies, the large-angle data become more and more sensitive to the real OP at sub-surface distances, and the DF3 potential clearly gives a much better OM description of the considered elastic $^{12}\text{C}+^{12}\text{C}$ data in comparison with the DF1 and DF2 potentials (see Figs. 5 and 6). The DF1 potential fails to account for both the oscillation pattern and magnitude of the measured elastic cross section at large angles. The use of the DF2 potential improves the agreement with the observed oscillation pattern data but

TABLE I: Parameters (9) of the WS imaginary OP for the elastic $^{12}\text{C}+^{12}\text{C}$ scattering at $E_{\text{lab}} = 16 - 117$ MeV. J_V is the volume integral (per interacting nucleon pair) of the DF3 real folded potential, J_W is that of the imaginary WS potential. σ_R is the total reaction cross section.

E_{lab} (MeV)	$-J_V$ (MeV fm ³)	W_V (MeV)	R_V (fm)	a_V (fm)	$-J_W$ (MeV fm ³)	σ_R (mb)	Ref.
16	368.9	2.136	6.560	0.208	17.7	369.0	[9]
18	368.5	2.228	6.514	0.252	18.2	507.8	[9]
20	368.1	2.660	6.472	0.204	21.2	603.3	[9]
35	365.2	3.227	6.711	0.218	28.7	1019.0	[29, 37]
45	363.2	3.543	6.532	0.232	29.1	1097.0	[29, 37]
74.2	357.6	8.533	6.509	0.412	71.1	1395.8	[31]
78.8	356.7	9.091	6.380	0.364	70.9	1335.2	[31]
83.3	355.8	8.672	6.367	0.387	67.5	1350.1	[31]
102.1	352.4	14.326	5.584	0.591	80.6	1395.8	[31]
117.1	349.6	15.770	5.536	0.590	86.6	1399.6	[31]

still fails to reproduce the magnitude of the cross sections. The DF3 potential (based on the realistic ADA for the overlap density) accounts very well for both the oscillation and magnitude of the measured elastic $^{12}\text{C}+^{12}\text{C}$ cross sections over the whole angular angle. As discussed earlier in the OM analyses of the low-energy elastic $^{12}\text{C}+^{12}\text{C}$ scattering [31, 65], the oscillation pattern and magnitude of the elastic angular distribution at the backward angles are sensitive to the elastic S matrix at low partial waves, which is determined by the scattering potential at small distances ($R \lesssim 4$ fm). Thus, we can conclude from the present OM study that the double-folded DF3 potential is the most realistic choice of the real OP for the $^{12}\text{C}+^{12}\text{C}$ system at low energies. The volume integral per interacting nucleon pair J_V of the DF3 potential (see Table I) also agrees consistently with that of the global OP for the $^{12}\text{C}+^{12}\text{C}$ system [38]. At the lowest energies considered here, the J_V value of the DF3 potential agrees closely with the empirical value of 360 ± 5 MeV fm³ of the deep WS potential that gives a good description of both the elastic scattering cross section and the underlying band of the $^{12}\text{C}+^{12}\text{C}$ resonances at low energies [41].

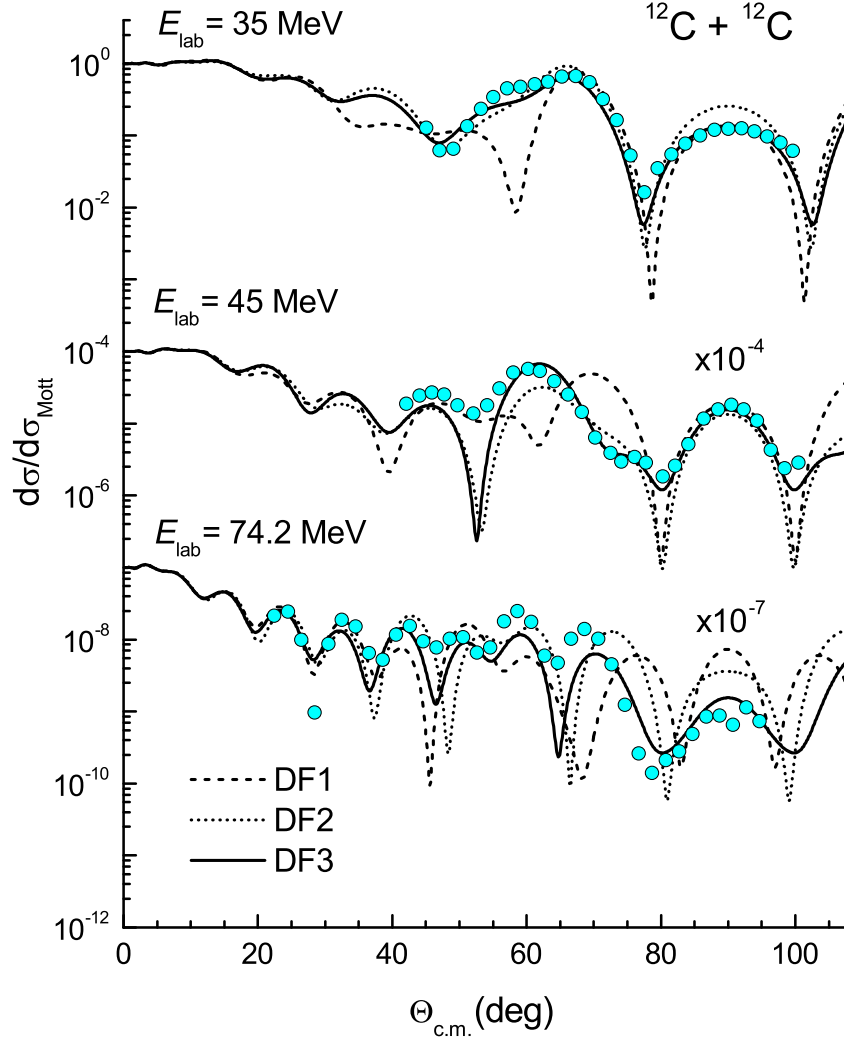


FIG. 5: The same as Fig. 4 but for the elastic $^{12}\text{C}+^{12}\text{C}$ scattering data at $E_{\text{lab}} = 35, 45,$ and 74.2 MeV [29, 37].

The boson symmetry of the identical $^{12}\text{C}+^{12}\text{C}$ system results naturally in the Mott oscillation of the elastic cross section at large angles (see Figs. 4-6), with a broad maximum located at $\theta_{\text{c.m.}} = 90^\circ$. Likely for this reason, the elastic excitation function for the elastic $^{12}\text{C}+^{12}\text{C}$ scattering was measured at 90° in several experiments [29, 31, 32, 37], at energies ranging from the Coulomb barrier up to above 10 MeV/nucleon. A complex structure of the peaks and valleys in the measured $^{12}\text{C}+^{12}\text{C}$ excitation function (see Fig. 7) was a puzzle during the 1980s, which was solved by McVoy and Brandan in their mean-field study of the elastic $^{12}\text{C}+^{12}\text{C}$ scattering [39]. Elastic $^{12}\text{C}+^{12}\text{C}$ scattering is known to exhibit a strongly refractive pattern, with the Airy structure of the nuclear rainbow well established at medium energies. As widely discussed in the literature, the elastic $^{12}\text{C}+^{12}\text{C}$ scattering data measured

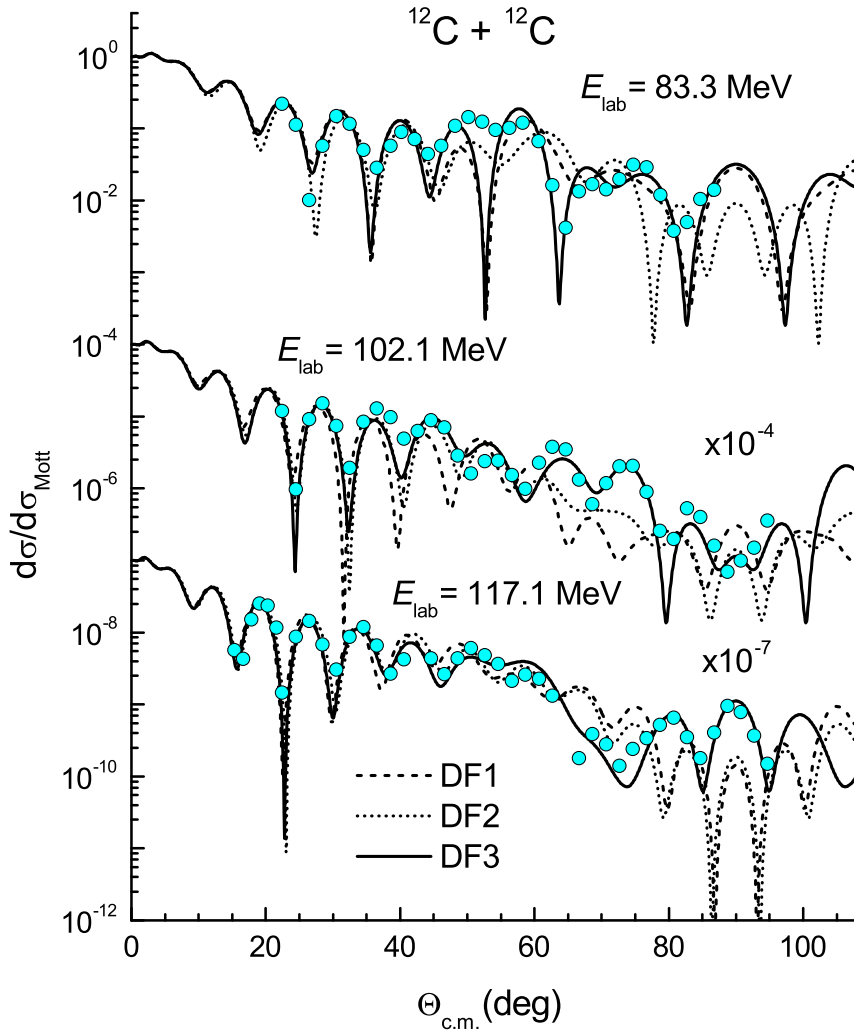


FIG. 6: The same as Fig. 4 but for the elastic $^{12}\text{C}+^{12}\text{C}$ scattering data at $E_{\text{lab}} = 83.3, 102.1,$ and 117.1 MeV [31].

at different energies, over a wide angular range, allow the determination of the real OP with much less ambiguity [40, 41, 47]. McVoy and Brandan have shown [39] that a continuous extrapolation of the deep family of the real OP determined by the nuclear rainbow scattering data down to lower energies shows that the uneven structure seen in the elastic $^{12}\text{C}+^{12}\text{C}$ excitation function measured at 90° is due to the evolution of the rainbow (Airy) pattern. In particular, the most prominent minimum at 102 MeV in the 90° excitation function was shown to be caused by the second Airy minimum passing through $\theta_{\text{c.m.}} \approx 90^\circ$ at that energy [39].

As can be seen in Fig. 6, the elastic $^{12}\text{C}+^{12}\text{C}$ scattering data measured at 102 MeV and

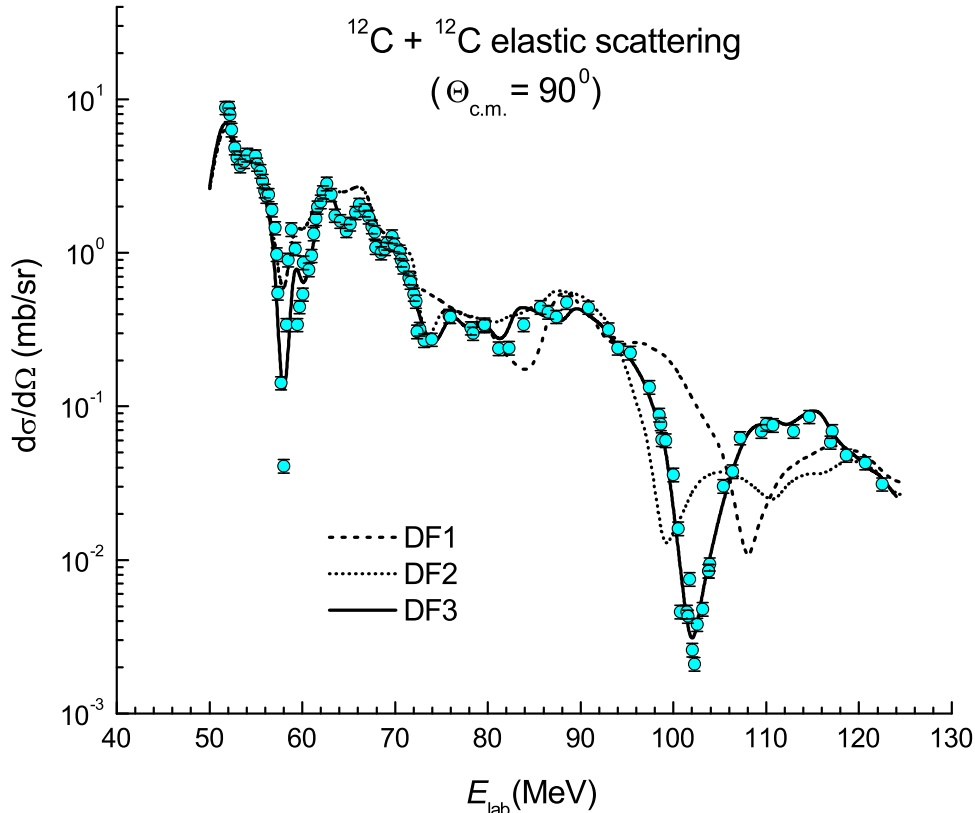


FIG. 7: Elastic $^{12}\text{C}+^{12}\text{C}$ excitation function [29, 31, 32, 37] measured at $\theta_{\text{c.m.}} = 90^\circ$ in comparison with the predictions given by three versions of the real OP considered in the present work. The same notation as that in Fig. 2 is used for the double-folded potential.

the two neighboring energies are consistently well reproduced only by the real folded DF3 potential. An OM calculation of the elastic $^{12}\text{C}+^{12}\text{C}$ scattering at 102 MeV, neglecting the boson symmetry, shows that the second Airy minimum A2 can be obtained at $\theta_{\text{c.m.}} \approx 90^\circ$ only with the DF3 potential. The three versions of the real OP discussed in the present work were used to calculate the 90° excitation function of the elastic $^{12}\text{C}+^{12}\text{C}$ scattering, using the WS imaginary OP with parameters extrapolated from those obtained at the energies considered in Figs. 3-6. One can see in Fig. 7 that only the DF3 potential is able to reproduce the measured 90° excitation function over a wide range of energies. The DF1 and DF2 potentials completely fail to account for the measured excitation function at energies of 80 to 120 MeV. Thus, we conclude that the present (low-energy) version of the DFM provides a reliable prediction of the real OP for the $^{12}\text{C}+^{12}\text{C}$ system at low energies. We expect, therefore, that this version of the DFM should be a suitable potential model for the

BPM study of $^{12}\text{C}+^{12}\text{C}$ fusion at astrophysical energies.

III. ASTROPHYSICAL S FACTOR OF $^{12}\text{C}+^{12}\text{C}$ FUSION

Given the vital role of the $^{12}\text{C}+^{12}\text{C}$ reaction rate in the carbon-burning process in massive stars [1, 2], numerous experimental and theoretical studies have been pursued during the last 40 years to assess the $^{12}\text{C}+^{12}\text{C}$ fusion reaction at low energies [5–25]. The typical temperature for $^{12}\text{C}+^{12}\text{C}$ fusion to occur in the carbon-oxygen core of a massive star ranges from about 0.6 to 1.0 GK, corresponding to the c.m. energy around the Gamow window centered at 1.5 MeV. With decreasing energy, the Coulomb repulsion becomes overwhelming and the direct measurement of the $^{12}\text{C}+^{12}\text{C}$ fusion cross section is extremely difficult. So far, one could go down in these experiments only to a energy of about 2.6 MeV [15, 24], where the absolute fusion cross section is a few nanobarns, with very large uncertainties. The uncertainties of the $^{12}\text{C}+^{12}\text{C}$ reaction rate were shown to affect strongly the astrophysical simulation of the nucleosynthesis in massive stars [3]. Very recently, the $^{12}\text{C}+^{12}\text{C}$ fusion cross section at energies lower than the Gamow energy was deduced indirectly from the measured $^{14}\text{N}+^{12}\text{C}$ reaction cross section [25] using the so-called Trojan horse method (THM). These indirect data show a very steep rise of the $^{12}\text{C}+^{12}\text{C}$ astrophysical factor with decreasing energy, where the resonant peak at around 0.9 MeV is larger than the empirical S factor extrapolated by Fowler *et al.* [4] by a factor of several thousands. Such a huge jump of the $^{12}\text{C}+^{12}\text{C}$ astrophysical S factor below the Gamow energy sparked off a strong debate on the use of the THM in this case [66, 67]. Moreover, the existing extrapolated $^{12}\text{C}+^{12}\text{C}$ astrophysical S factors based on the measured fusion data seem to diverge at the lowest energies. While the extrapolation by Fowler *et al.* [4] gives a steady rise of the S factor with decreasing energy, an opposite scenario was suggested by Jiang *et al.* [17, 24] which favors the hindrance of $^{12}\text{C}+^{12}\text{C}$ fusion near the Gamow window and a strong decrease of the S factor with decreasing energy. It is, therefore, highly desirable to have a reliable mean-field prediction of the $^{12}\text{C}+^{12}\text{C}$ astrophysical S factor at low energies, which should be helpful in narrowing the uncertainties as well as predicting the S factor at very low energies, currently beyond reach by direct measurement of $^{12}\text{C}+^{12}\text{C}$ fusion.

In the BPM, the probability of the $^{12}\text{C}+^{12}\text{C}$ reaction is determined essentially by the tunnel effect that allows two ^{12}C nuclei to penetrate the Coulomb barrier at c.m. energy E

below the barrier height. Given the Q value of $^{12}\text{C}+^{12}\text{C}$ fusion of nearly 14 MeV, $^{12}\text{C}+^{12}\text{C}$ reactions can proceed through different configurations of ^{24}Mg , and it is quite complicated to take all these reaction channels into account properly in the coupled reaction channel calculation. A nice feature of the mean-field description of the $^{12}\text{C}+^{12}\text{C}$ interaction is that the total $^{12}\text{C}+^{12}\text{C}$ fusion cross section can be simply determined as a coherent sum of all partial-wave contributions of the $^{12}\text{C}+^{12}\text{C}$ transmission:

$$\sigma_{\text{fus}} = \frac{\pi}{k^2} \sum_{l=0}^{\infty} [1 + (-1)^l] (2l + 1) T_l, \quad (10)$$

where we have taken into account the boson symmetry of the total wave function of the two identical ^{12}C nuclei. k is the relative-motion momentum and l is the orbital angular momentum of the dinuclear system. The l -dependent transmission coefficient T_l gives the probability of the two nuclei to penetrate through the potential barrier built up from the *attractive* nuclear potential and *repulsive* Coulomb and centrifugal potentials as

$$V_l(R) = V_{\text{N}}(R) + V_{\text{C}}(R) + \frac{\hbar^2 l(l+1)}{2\mu R^2}. \quad (11)$$

To explore the mean-field aspect of $^{12}\text{C}+^{12}\text{C}$ fusion, three versions of the double-folded potential given by the DFM approach (2)-(7) have been used as the nuclear potential V_{N} . For consistency, the same folded Coulomb potential V_{C} as that obtained in the folding calculation (4) was used to determine the total potential (11). Thus, the height and location of the potential barrier are rigorously predicted by our DFM approach for the BPM study of $^{12}\text{C}+^{12}\text{C}$ fusion.

For all partial waves l with the corresponding potential barrier lying below the c.m. energy of the dinuclear system ($V_{\text{Bl}} < E$), the transmission coefficient T_l is readily obtained using the Hill-Wheeler formula [69] as

$$T_l = \left\{ 1 + \exp \left[\frac{2\pi(V_{\text{Bl}} - E)}{\hbar\omega_l} \right] \right\}^{-1}, \quad (12)$$

where $\hbar\omega_l$ is the curvature of the total potential (11) at the barrier top:

$$\hbar\omega_l = \left| \frac{\hbar^2}{\mu} \frac{d^2 V_l(R)}{dR^2} \right|_{R=R_{\text{Bl}}}^{1/2} \quad \text{with } V_{\text{Bl}} = V_l(R = R_{\text{Bl}}). \quad (13)$$

For all partial waves l with $V_{\text{Bl}} > E$, we used the transmission coefficient given by the WKB approximation [2] to determine the total transmission coefficient of tunneling through

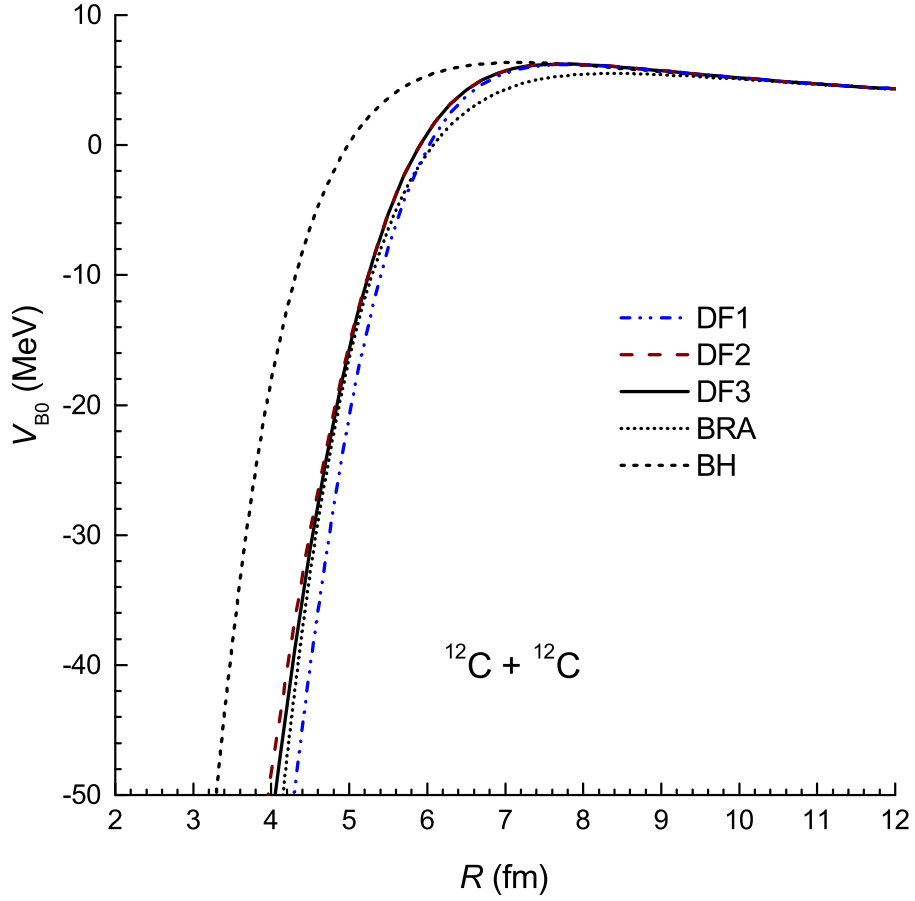


FIG. 8: Potential barrier V_B at $l = 0$ given by the double-folded DF1, DF2, and DF3 potentials, in comparison with that given by the energy-dependent WS potential (BRA) suggested by Brandan *et al.* [38], and phenomenological potential (BH) used by Buck and Hopkins in the $^{12}\text{C}+^{12}\text{C}$ cluster model [68].

the barrier [70] as

$$T_l = \frac{T_l^{\text{WKB}}}{1 + T_l^{\text{WKB}}} \text{ with } T_l^{\text{WKB}} = \exp \left\{ -\frac{2}{\hbar} \int_{R_1}^{R_2} \sqrt{2\mu[V_l(R) - E]} dR \right\}. \quad (14)$$

Here R_1 and R_2 are the inner and outer turning points $V_l(R_1) = V_l(R_2) = E$. Because the fusion cross section decreases too rapidly with the decreasing energy, it is convenient to consider the astrophysical S -factor, determined as

$$S(E) = E\sigma_{\text{fus}}(E) \exp(2\pi\eta), \quad (15)$$

where the Sommerfeld parameter $\eta = Z_1 Z_2 e^2 / \hbar v$, and v is the relative velocity of the

dinuclear system.

It is obvious that the most vital input for the BPM is the choice of the nuclear potential (11). To illustrate this effect, we have used in the present work two more potential models for comparison with the double-folded potentials. The first is the energy-dependent WS potential parametrized by Brandan *et al.* [38] for the OM study elastic $^{12}\text{C}+^{12}\text{C}$ scattering at energies below 6 MeV/nucleon, denoted hereafter as the BRA potential. The second choice is the energy-independent potential parametrized by Buck and Hopkins [68] for a proper description of the g.s. band of ^{24}Mg in the $^{12}\text{C}+^{12}\text{C}$ cluster model, denoted hereafter as the BH potential. The potential barrier at zero angular momentum given by different nuclear potentials obtained at $E = 3$ MeV is shown in Fig. 8. We note that the energy dependence of the folded and BRA potentials are quite weak at $E \approx 2 - 8$ MeV, and the barrier height and position remain practically the same over this energy range as those shown in Fig. 8. In comparison with the results of the earlier BPM analyses of $^{12}\text{C}+^{12}\text{C}$ fusion where the empirical barrier height $V_{\text{B}0} \approx 6.2 - 6.3$ MeV and position $R_{\text{B}} \approx 7.4 - 7.6$ fm were deduced from the best BPM fit to the measured σ_{fus} [12], only the barrier height and position given by the double-folded potentials ($V_{\text{B}} \approx 6.2$ MeV and $R_{\text{B}} \approx 7.8$ fm) agree reasonably with the empirical systematics. The agreement is worse for those obtained with the BRA potential ($V_{\text{B}} \approx 5.5$ MeV and $R_{\text{B}} \approx 8.4$ fm) and BH potential ($V_{\text{B}} \approx 6.4$ MeV and $R_{\text{B}} \approx 7.2$ fm). Because R_{B} is larger than the grazing radius of 6 fm used in the ADA for the overlap density (8), the two versions DF2 and DF3 of the double-folded potential give about the same barrier height at $R_{\text{B}} \approx 7.8$ fm. The DF1 potential is more attractive at the surface, and gives a lower barrier at $R \approx 4 - 7$ fm compared to that given by the DF2 and DF3 potentials.

The difference in the potential barrier given by different potential models can be seen in the calculated $^{12}\text{C}+^{12}\text{C}$ fusion cross sections shown in Fig. 9. The barrier given by the BH potential is slightly higher and wider than those given by the double-folded and BRA potentials, and that results in a weaker tunneling. Therefore, the $^{12}\text{C}+^{12}\text{C}$ fusion cross section given by the BH potential underestimates the measured fusion cross section over the whole energy range. In contrast, the BRA potential generates a lower barrier which leads to a significantly larger fusion cross section compared with the measured data. Without any readjustment of the potential strength ($N_{\text{R}} = 1$), the three double-folded potentials well reproduce the measured $^{12}\text{C}+^{12}\text{C}$ fusion cross section over 11 orders of magnitude, as shown

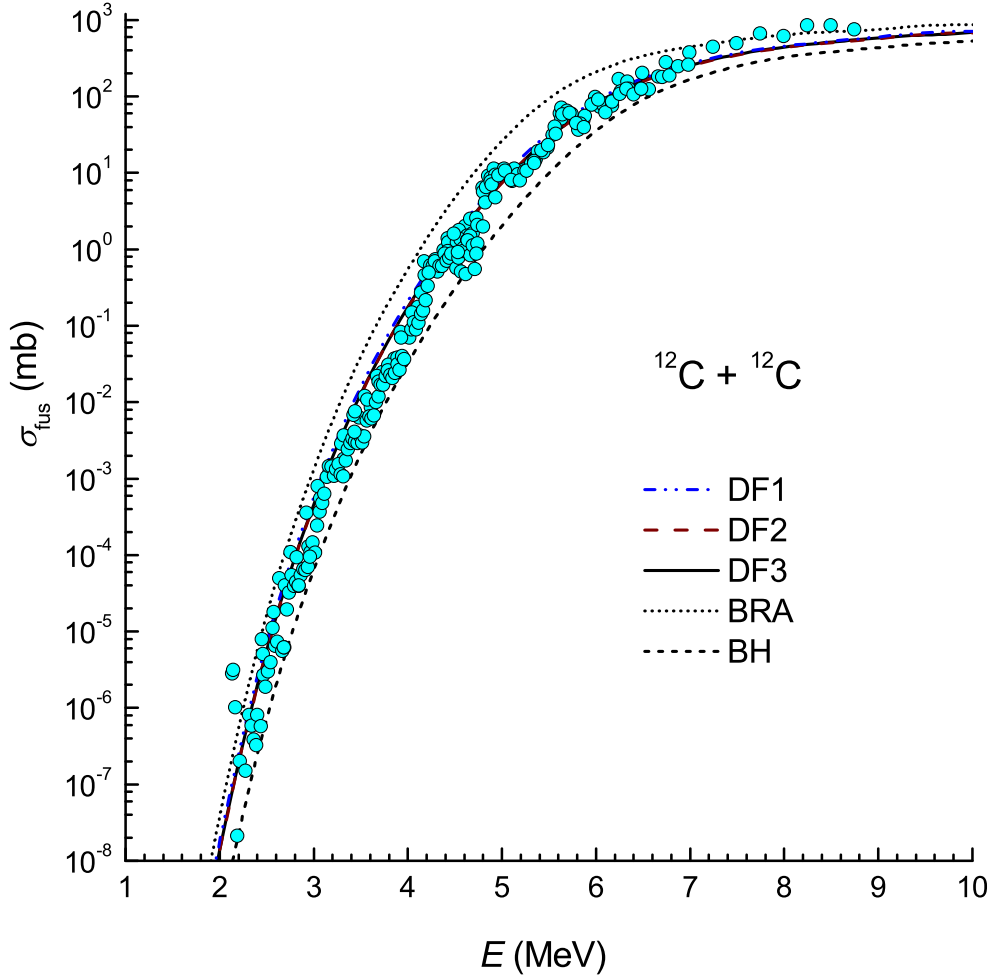


FIG. 9: $^{12}\text{C}+^{12}\text{C}$ fusion cross section given by the BPM using the double-folded DF1, DF2, and DF3 potentials, BRA potential [38], and BH potential [68], in comparison with the data [5–7, 11, 12, 24] from the direct measurement of the $^{12}\text{C}+^{12}\text{C}$ fusion at energies of 2-9 MeV.

in Fig. 9. The difference between the potential barrier given by the DF1 potential and those given by the DF2 and DF3 potentials can be seen only in the astrophysical S factors shown in Fig. 10. Combining with a good OM description of the elastic $^{12}\text{C}+^{12}\text{C}$ scattering at low energies discussed in Sec. II, the results shown in Fig. 9 confirm the validity of the low-energy version of the DFM using the realistic adiabatic approximation (8) for the overlap density.

The astrophysical S factors (15) of $^{12}\text{C}+^{12}\text{C}$ fusion obtained with the calculated and measured cross sections shown in Fig. 9 are shown in Fig. 10 together with the phenomenological S factor suggested by Fowler *et al.* [4], based on the “black body” model using a

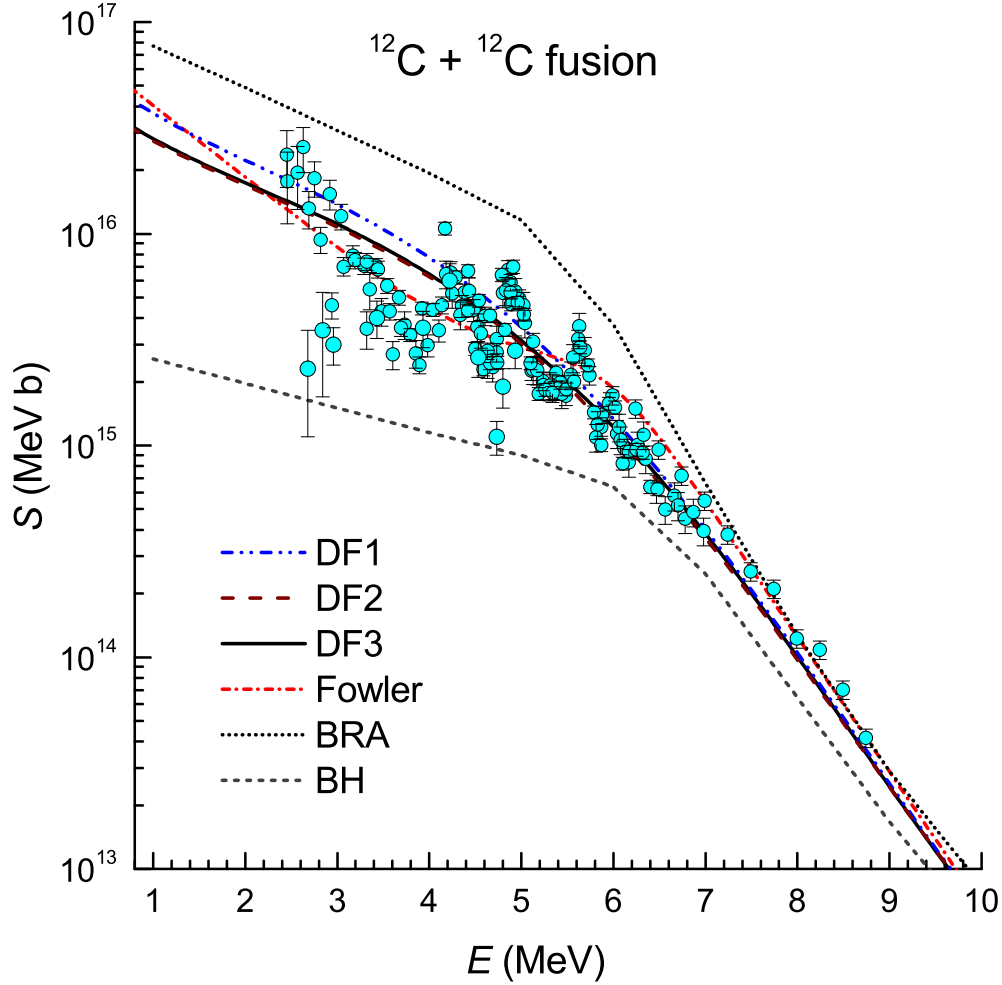


FIG. 10: Astrophysical S -factors of $^{12}\text{C}+^{12}\text{C}$ fusion predicted by the BPM using the same potential models as those used to obtain the fusion cross sections shown in Fig. 9, in comparison with the phenomenological S -factor suggested by Fowler *et al.* [4] and the data from direct measurements of the $^{12}\text{C}+^{12}\text{C}$ fusion taken from Refs. [5–7, 11, 12, 24].

phenomenological nuclear potential with parameters adjusted by the best BPM fit to the data of the direct measurements of $^{12}\text{C}+^{12}\text{C}$ fusion. Because of the ongoing debate on the THM [66, 67] and the resulting uncertainty of recent data [25] from indirect measurement of $^{12}\text{C}+^{12}\text{C}$ fusion, these data were not included in the present discussion. One can see in Fig. 10 the well established resonant behavior of the S factor deduced from the measured $^{12}\text{C}+^{12}\text{C}$ fusion cross section at energies below 6 MeV, which remains still an unsolved problem for microscopic studies of $^{12}\text{C}+^{12}\text{C}$ fusion. The non-resonant strength of the observed S

factor (sometimes referred to as the background excitation function [12]) is well described by the double-folded DF2 and DF3 potentials. The S factor obtained with the double-folded potentials also agrees reasonably with the phenomenological S factor extrapolated by Fowler *et al.*, except at the lowest energies ($E < 1$ MeV) where our mean-field result (given by the DF2 and DF3 potentials) is lower than that given by Fowler's extrapolation by a factor of 2. The discrepancy between the S factors obtained with the BRA and BH potentials and the experimental data is quite large and keeps increasing with decreasing energies, up to the factor of 10 at low energies. This result shows clearly that astrophysical S factor of $^{12}\text{C}+^{12}\text{C}$ fusion at the sub-barrier energies is strongly sensitive to the shape and height of the potential barrier, and the measured S factor is not only important for the astrophysical studies but also provides a good test ground for the potential model of the $^{12}\text{C}+^{12}\text{C}$ interaction at low energies.

The fact that the mean-field based DFM has stood the test and provides consistently a good description of both the elastic $^{12}\text{C}+^{12}\text{C}$ scattering at low energies and non-resonant behavior of the astrophysical S factor of $^{12}\text{C}+^{12}\text{C}$ fusion is an important result. We recall that the (G-matrix based) density dependent CDM3Y3 interaction was parametrized some 20 years ago [44] to reproduce the saturation properties of nuclear matter and nuclear incompressibility $K \approx 217$ MeV. Added by the correction from the rearrangement term (6) deduced in the recent HF study of nuclear matter [51], the CDM3Y3 interaction has been used in the DFM to give an accurate prediction of the real OP for the $^{12}\text{C}+^{12}\text{C}$ system at refractive energies [48]. Now, this same DFM approach with a proper adiabatic treatment of the overlap density (8) also describes very well the real OP at low energies and the fusion cross section for the $^{12}\text{C}+^{12}\text{C}$ system. This suggests naturally a strong mean-field dynamics of the $^{12}\text{C}+^{12}\text{C}$ reaction at low energies. The resonant structures observed in the $^{12}\text{C}+^{12}\text{C}$ fusion cross section should be treated, therefore, as strong fluctuations beyond the mean field. A coupled reaction channel study of the involved reactions $^{12}\text{C}(^{12}\text{C},p)^{23}\text{Na}$, $^{12}\text{C}(^{12}\text{C},\alpha)^{20}\text{Ne}$, and $^{12}\text{C}(^{12}\text{C},n)^{23}\text{Mg}$, using the (diagonal) optical potentials given by the present low-energy version of the DFM, should be of interest to assess the contribution from these reaction channels [2] to the total $^{12}\text{C}+^{12}\text{C}$ fusion.

For possible use of the mean-field based astrophysical S factor of $^{12}\text{C}+^{12}\text{C}$ fusion in the astrophysical calculation, we have parametrized the S factor given by the double-folded DF3

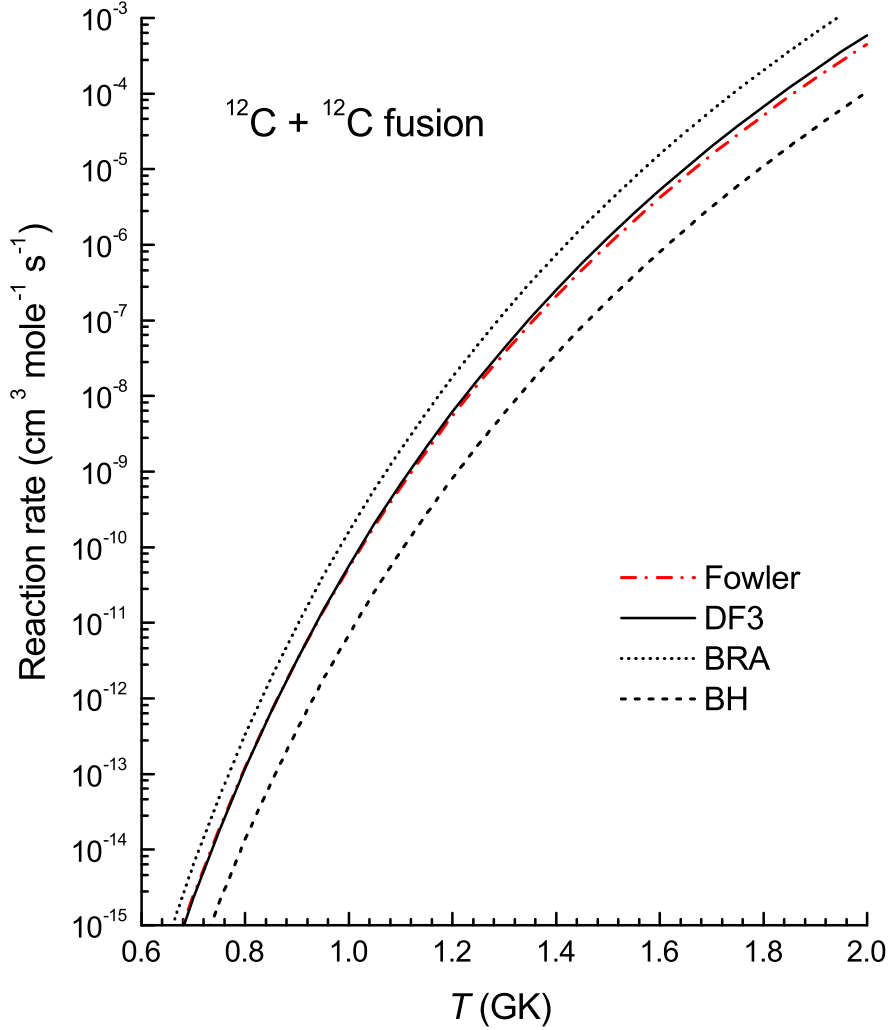


FIG. 11: Reaction rates (17) of $^{12}\text{C}+^{12}\text{C}$ fusion obtained from the S factors given by the double-folded DF3, BRA, and BH potentials in comparison with that obtained from the phenomenological S factor suggested by Fowler *et al.* [4].

potential in the following analytical form:

$$S(E) = 10^{a_0} + a_1 E + a_2 E^2 + a_3 E^3. \quad (16)$$

Here the energy E is given in MeV, $a_0 = 16.75 \pm 0.04$, $a_1 = -0.33 \pm 0.03 \text{ MeV}^{-1}$, $a_2 = 0.048 \pm 0.009 \text{ MeV}^{-2}$, and $a_3 = -0.0065 \pm 0.0007 \text{ MeV}^{-3}$, which give the S factor in MeV b. Ultimately, the quantity that is widely used in astrophysical studies of stellar evolution and nucleosynthesis is the nuclear *reaction rate*. In general, the reaction rate for a fusion pair at

the given temperature T is determined [2] from the astrophysical S factor as

$$N_A \langle \sigma v \rangle = \left(\frac{8}{\pi \mu} \right)^{1/2} \frac{N_A}{(kT)^{3/2}} \int_0^\infty S(E) \exp(-2\pi\eta - \frac{E}{kT}) dE, \quad (17)$$

where N_A and k are the Avogadro and Boltzmann constants, respectively. With the temperature T and energy E given in GK and MeV, the reaction rate (17) is obtained in $\text{cm}^3 \text{mole}^{-1} \text{s}^{-1}$. The reaction rates (17) of the $^{12}\text{C}+^{12}\text{C}$ fusion obtained from the S factors given by the three potential models are shown in Fig. 11 together with the reaction rate obtained from the phenomenological S -factor extrapolated by Fowler *et al.* [4]. One can see that the reaction rate obtained with the double-folded DF3 potential is quite close to that given by the S -factor extrapolated by Fowler, especially in the low temperature range of 0.6 to 1 GK that covers the Gamow window. The impact by the barrier height and its location on the reaction rate is very strong; we found that the reaction rate obtained with the BH potential is of 7.5 to 10 times lower than that obtained with the DF3 potential. In contrast, the reaction rate obtained with the BRA potential is larger than that given by the DF3 potential by a factor of 2.5 to 3 in the same temperature range. The results shown in Fig. 11 confirm again the importance of a proper choice of the potential model for the study of $^{12}\text{C}+^{12}\text{C}$ fusion. The ignition of carbon burning might take place at a higher temperature if the extrapolation of the S factor based on a hindrance of the $^{12}\text{C}+^{12}\text{C}$ fusion near and below the Gamow window is chosen [17, 24], which gives a reaction rate several times lower than that suggested by Fowler *et al.* (see Fig. 6 of Ref. [24] and the discussion therein).

IV. SUMMARY

The mean-field based CDM3Y3 density dependent interaction [44], well tested in HF studies of nuclear matter [47] and the nucleon mean-field potential [51], has been used in an extended DFM approach [48] to calculate the real OP for elastic $^{12}\text{C}+^{12}\text{C}$ scattering at low energies. To validate the use of the DFM at low energies, a realistic adiabatic approximation (8) for the $^{12}\text{C}+^{12}\text{C}$ overlap density has been suggested to replace the FDA normally used in DFM calculation at energies above 10 MeV/nucleon. Without any renormalization of its strength, the real double-folded DF3 potential (obtained with the ADA for the overlap density and used with the best-fit imaginary WS potential) accounts very well for the elastic $^{12}\text{C}+^{12}\text{C}$ cross sections measured over a wide angular angle, at different energies. The FDA

for the overlap density was found to be inappropriate for DFM calculation of the nucleus-nucleus OP at low energies.

The double-folded DF3 potential was also shown to fit well into the deep family of the mean-field potential at low energies suggested some 25 years ago for the $^{12}\text{C}+^{12}\text{C}$ system by McVoy and Brandan [39] that properly explains the structure observed in the 90° elastic $^{12}\text{C}+^{12}\text{C}$ excitation function as being due to the evolution of the nuclear rainbow. Especially, from the three versions of the double-folded potential considered in the present work, only the DF3 potential is capable of reproducing the prominent minimum of the 90° excitation function at $E_{\text{lab}} = 102$ MeV, caused by the second Airy minimum passing through $\theta_{\text{c.m.}} \approx 90^\circ$ at that particular energy [39].

The present low-energy version of the DFM is further used to calculate the nuclear potential for the BPM study of the astrophysical S factor of $^{12}\text{C}+^{12}\text{C}$ fusion. Without any free parameter, the double-folded potential accounts very well for the non-resonant strength of the $^{12}\text{C}+^{12}\text{C}$ astrophysical S factor, in a close agreement with that given by the phenomenological parametrization by Fowler *et al.* [4]. Together with the DFM, another two potential models for the $^{12}\text{C}+^{12}\text{C}$ interaction [38, 68] were also used in the present work to emphasize the sensitivity of the calculated S factor to the height and position of the potential barrier. A consistently good description of both the elastic scattering and fusion data by the double-folded DF3 potential suggests a strong mean-field dynamics of the $^{12}\text{C}+^{12}\text{C}$ reaction at low energies.

Although the simultaneous OM analysis of both the elastic $^{12}\text{C}+^{12}\text{C}$ scattering and fusion has been performed earlier using other models (see, e.g., Ref. [14]), this is the first time that a mean-field based density dependent NN interaction, which gives a realistic HF description of the saturation properties of nuclear matter [51], has been successfully used in a HF-type folding model calculation of the OP for a consistent study of low-energy elastic $^{12}\text{C}+^{12}\text{C}$ scattering and fusion. Given the significant coupled channel effects shown earlier in the study of elastic $^{12}\text{C}+^{12}\text{C}$ scattering and fusion [21], the double-folded DF3 potential can be used as the reliable input for the real OP in a coupled reaction channels study of the $^{12}\text{C}+^{12}\text{C}$ scattering and fusion, to explore the explicit contributions from the involved reaction channels [2] to the total $^{12}\text{C}+^{12}\text{C}$ fusion and their possible role in shaping the resonances observed in the experimental S factor at energies of 2 to 6 MeV.

Acknowledgments

We thank the authors of Ref. [56] for providing us with the nuclear density of ^{12}C given by the microscopic NCSM calculation. The present research has been supported, in part, by the National Foundation for Scientific and Technological Development (NAFOSTED Project No. 103.04-2017.317).

-
- [1] W.A. Fowler, *Rev. Mod. Phys.* **56**, 149 (1984).
 - [2] C. Iliadis, *Nuclear Physics of Stars* (Wiley-VCH Press, Weinheim, 2015).
 - [3] M.E. Bennett, R. Hirschi, M. Pignatari, S. Diehl, C. Fryer, F. Herwig, A. Hungerford, K. Nomoto, G. Rockefeller, F.X. Timmes, and M. Wiescher, *Mon. Not. R. Astron. Soc.* **420**, 3047 (2012).
 - [4] W.A. Fowler, G.R. Caughlan, and B.A. Zimmerman, *Annu. Rev. Astron. Astrophys.* **13**, 69 (1975).
 - [5] J.A. Patterson, H. Winkler, and C.S. Zaidins, *Astrophys. J.* **157**, 367 (1969).
 - [6] M.G. Mazarakis and W.E. Stephens, *Phys. Rev. C* **7**, 1280 (1973).
 - [7] M.D. High and B. Čujec, *Nucl. Phys. A* **282**, 181 (1977).
 - [8] K.U. Kettner, H. Lorenz-Wirzba, and C. Rolfs, *Z. Phys. A* **298**, 65 (1980).
 - [9] W. Treu, H. Fröhlich, W. Galster, P. Dück, and H. Voit, *Phys. Rev. C* **22**, 2462 (1980).
 - [10] H.W. Becker, K.U. Kettner, C. Rolfs, and H.P. Trautvetter, *Z. Phys. A* **303**, 305 (1981).
 - [11] B. Dasmahapatra, B. Čujec, and F. Lahlou, *Nucl. Phys. A* **384**, 257 (1982).
 - [12] E.F. Aguilera *et al.*, *Phys. Rev. C* **73**, 064601 (2006).
 - [13] L. Barrón-Palos *et al.*, *Nucl. Phys. A* **779**, 318 (2006).
 - [14] L.R. Gasques, A.V. Afanasjev, E.F. Aguilera, M. Beard, L.C. Chamon, P. Ring, M. Wiescher, and D.G. Yakovlev, *Phys. Rev. C* **72**, 025806 (2005).
 - [15] T. Spillane *et al.*, *Phys. Rev. Lett.* **98**, 122501 (2007).
 - [16] B. Bucher *et al.*, *Phys. Rev. Lett.* **114**, 251102 (2015).
 - [17] C.L. Jiang, K.E. Rehm, B.B. Back, and R.V.F. Janssens, *Phys. Rev. C* **75**, 015803 (2007).
 - [18] V.Yu. Denisov and N.A. Pilipenko, *Phys. Rev. C* **81**, 025805 (2010).
 - [19] M. Notani *et al.*, *Phys. Rev. C* **85**, 014607 (2012).

- [20] C.L. Jiang, B.B. Back, H. Esbensen, R.V.F. Janssens, K.E. Rehm, and R.J. Charity, Phys. Rev. Lett. **110**, 072701 (2013).
- [21] M. Assunção and P. Descouvemont, Phys. Lett. B **723**, 355 (2013).
- [22] A.A. Aziz, N. Yusof, M.Z. Firihi, and H.A. Kassim, Phys. Rev. C **91**, 015811 (2015).
- [23] S. Courtin *et al.*, in Proceedings of the 14th International Symposium on Nuclei in the Cosmos (NIC2016) [JPS Conf. Proc. **14**, 021001 (2017)].
- [24] C.L. Jiang *et al.*, Phys. Rev. C **97**, 012801(R) (2018).
- [25] A. Tumino *et al.*, Nature (London) **557**, 687 (2018).
- [26] C.Y. Wong, Phys. Rev. Lett. **31**, 766 (1973).
- [27] K. Hagino and N. Takigawa, Prog. Theor. Phys. **128**, 1061 (2012).
- [28] B.B. Back, H. Esbensen, C.L. Jiang, and K.E. Rehm, Rev. Mod. Phys. **86**, 317 (2014).
- [29] W. Reilly, R. Wieland, A. Gobbi, M.W. Sachs, J. Maher, R.H. Siemssen, D. Mingay, and D.A. Bromley, Nuovo Cimento A **13**, 913 (1973).
- [30] E.R. Cosman, T.M. Cormier, K. Van Bibber, A. Sperduto, G. Young, J. Erskine, L.R. Greenwood, and O. Hansen, Phys. Rev. Lett. **35**, 265 (1975).
- [31] R.G. Stokstad, R.M. Wieland, G.R. Satchler, C.B. Fulmer, D.C. Hensley, S. Raman, L.D. Rickertsen, A.H. Snell, and P.H. Stelson, Phys. Rev. C **20**, 655 (1979).
- [32] A. Morsad, F. Haas, C. Beck, and R.M. Freeman, Z. Phys. A **338**, 61 (1991).
- [33] M. Aliotta, S. Cherubini, E. Costanzo, M. Lattuada, S. Romano, D. Vinciguerra, and M. Zadro, Z. Phys. A **353**, 43 (1995).
- [34] C.A. Bremner *et al.*, Phys. Rev. C **66**, 034605 (2002).
- [35] J.V. Maher, M.W. Sachs, R.H. Siemssen, A. Weidinger, and D.A. Bromley, Phys. Rev. **188**, 1665 (1969).
- [36] A. Gobbi, R. Wieland, L. Chua, D. Shapira, and D.A. Bromley, Phys. Rev. C **7**, 30 (1973).
- [37] W. Reilly, R. Wieland, A. Gobbi, M.W. Sachs, and D.A. Bromley, Nuovo Cimento A **13**, 897 (1973).
- [38] M.E. Brandan, M. Rodríguez-Villafuerte, and A. Ayala, Phys. Rev. C **41**, 1520 (1990).
- [39] K.W. McVoy and M.E. Brandan, Nucl. Phys. A **542**, 295 (1992).
- [40] M.E. Brandan and G.R. Satchler, Phys. Rep. **285**, 143 (1997).
- [41] Y. Kondō, M.E. Brandan, and G.R. Satchler, Nucl. Phys. A **637**, 175 (1998).
- [42] G.R. Satchler and W.G. Love, Phys. Rep. **55**, 183 (1979).

- [43] D.T. Khoa, W. von Oertzen, and H.G. Bohlen, Phys. Rev. C **49**, 1652 (1994).
- [44] D.T. Khoa, G.R. Satchler, and W. von Oertzen, Phys. Rev. C **56**, 954 (1997).
- [45] D.T. Khoa and G.R. Satchler, Nucl. Phys. A **668**, 3 (2000).
- [46] D.T. Khoa, Phys. Rev. C **63**, 034007 (2001).
- [47] D.T. Khoa, W. von Oertzen, H.G. Bohlen, and S. Ohkubo, J. Phys. G **34**, R111 (2007).
- [48] D.T. Khoa, N.H. Phuc, D.T. Loan, and B.M. Loc, Phys. Rev. C **94**, 034612 (2016).
- [49] I. Reichstein and F.B. Malik, Phys. Lett. B **37**, 344 (1971).
- [50] I. Reichstein and F.B. Malik, Ann. Phys. (N.Y.) **98**, 322 (1976).
- [51] D.T. Loan, B.M. Loc, and D.T. Khoa, Phys. Rev. C **92**, 034304 (2015).
- [52] J.E. Poling, E. Norbeck, and R.R. Carlson, Phys. Rev. C **13**, 648 (1976).
- [53] N. Anantaraman, H. Toki, and G.F. Bertsch, Nucl. Phys. A **398**, 269 (1983).
- [54] P.H. Heenen and M.R. Godefroid, Scholarpedia **7**, 10545 (2012).
- [55] P.E. Hodgson, Rep. Prog. Phys. **38**, 847 (1975).
- [56] M. Gennari, M. Vorabbi, A. Calci, and P. Navrátil, Phys. Rev. C **97**, 034619 (2018).
- [57] J. Raynal, *Computing as a Language of Physics* (IAEA, Vienna, 1972) p. 75; coupled-channel code ECIS97 (unpublished).
- [58] K. Siwek-Wilczyńska and J. Wilczyński, Phys. Rev. C **64**, 024611 (2001).
- [59] T. Ichikawa, K. Hagino, and A. Iwamoto, Phys. Rev. Lett. **103**, 202701 (2009).
- [60] Y. Taniguchi, Y. Kanada-En'yo, and T. Suhara, Prog. Theor. Exp. Phys. **2013**, 043D04.
- [61] T. Ichikawa, Phys. Rev. C **92**, 064604 (2015).
- [62] N. Ohtsuka, R. Linden, A. Faessler, and F.B. Malik, Nucl. Phys. A **465**, 550 (1987).
- [63] S. Goriely, M. Samyn, and J.M. Pearson, Phys. Rev. C **75**, 064312 (2007).
- [64] Y. Kucuk and I. Boztosun, Nucl. Phys. A **764**, 160 (2006).
- [65] N. Rowley, H. Doubre, and C. Marty, Phys. Lett. B **69**, 147 (1977).
- [66] A.M. Mukhamedzhanov and D.Y. Pang, arXiv:1806.08828.
- [67] A. Tumino *et al.*, arXiv:1807.06148.
- [68] B. Buck, P.D.B. Hopkins, and A.C. Merchant, Nucl. Phys. A **513**, 75 (1990).
- [69] D.L. Hill and J.A. Wheeler, Phys. Rev. **89**, 1102 (1953).
- [70] P. Fröbrich and R. Lipperheide, *Theory of Nuclear Reactions*, Clarendon, Oxford (1996).